Chemical Engineering Journal 290 (2016) 1–11

Contents lists available at ScienceDirect

Chemical Engineering Journal

journal homepage: www.elsevier.com/locate/cej

Highly effective removal of Cu(II) by a novel 3-aminopropyltriethoxysilane functionalized polyethyleneimine/sodium alginate porous membrane adsorbent

Xue Sun [a], Jian Hua Chen [a,b,*], Zhenbo Su [a], Yihong Huang [a], Xinfei Dong [a]

[a] College of Chemistry and Environmental, Minnan Normal University, Zhangzhou 363000, China
[b] Fujian Province University Key Laboratory of Modern Analytical Science and Separation Technology, Minnan Normal University, Zhangzhou 363000, China

HIGHLIGHTS

- Adsorption capacity of the PEI/SA was 7 times more than that of pristine SA membrane.
- The PEI/SA showed excellent adsorption selectivity for Cu(II) ions.
- The adsorption rate was very fast, and adsorption equilibrium time was 60 min.
- Reusability of the PEI/SA was excellent.
- The PEI/SA is an easy operation and efficient adsorbent for removal Cu(II) ions.

ARTICLE INFO

Article history:
Received 5 September 2015
Received in revised form 29 December 2015
Accepted 30 December 2015
Available online 11 January 2016

Keywords:
Sodium alginate
Polyethyleneimine
Porous membrane
Adsorption
Cu(II)

ABSTRACT

In the present paper, we prepared a novel porous membrane adsorbent (PEI/SA) by immobilizing polyethyleneimine (PEI) with sodium alginate (SA), then further functionalized PEI/SA with 3-aminopropyltriethoxysilane and tested its adsorption performance for removing Cu(II). To investigate the adsorption kinetics of Cu(II) onto this newly developed PEI/SA, we performed a series of batch experiments under various conditions: solution pH, adsorbent dose, initial Cu(II) concentration, adsorption temperature, and contact time. The results show that the maximum adsorption capacity of Cu(II) onto the PEI/SA is approximate 329.8 mg/g, which is 7 times more than that of pristine SA porous membrane. We also examined the Lagergren pseudo-first-order and pseudo-second-order kinetic models, the intraparticular diffusion model, and the Crank model to study the mechanism of adsorption process. Kinetics experiments indicate that the pseudo-second-order model displays the best correlation with adsorption kinetics data. The Crank model shows that the intra-particle solute diffusion is the main rate-controlling step. Furthermore, our adsorption equilibrium data could be better described by the Freundlich equation. Effect of ionic strength on adsorption process is weakly. Co-existing Cd(II), Ni(II) and Cr(VI) ions hardly affect the adsorption capacity of PEI/SA towards Cu(II). The reusability experiments show that the PEI/SA has excellent adsorption–desorption efficiencies. The results indicate that the prepared PEI/SA is promising for Cu(II) removal, from the viewpoints of low cost and easy operation.

1. Introduction

Recently, rapid industrialization throughout the world has caused the release of various pollutants including heavy metals and organic substances into environment. Unlike most organic wastes, heavy metals are non-biodegradable and can be accumulated in living tissues, causing various diseases and disorders. Heavy metal ions and their toxic effects have become a major world problem. As a result, environment contamination causing by heavy metal ions has received extensive attention throughout the world. Among various heavy metals, Cu(II) and copper containing materials have number of applications including manufacturing of copper water pipes and brass radiators, as a constituent of fertilizers, pesticides, fireworks and antifouling paints applied on ship hulls [1]. Copper is one of the elements which is essential for human beings, but at higher concentration it affects the health of fauna, flora and humans adversely. Due to the toxicity

* Corresponding author at: College of Chemistry and Environmental, Minnan Normal University, Zhangzhou 363000, China. Tel.: +86 596 2591445; fax: +86 596 2520035.
E-mail address: jhchen73@126.com (J.H. Chen).

http://dx.doi.org/10.1016/j.cej.2015.12.106
1385-8947/

of copper, the recommendation of the World Health Organization for the safe amount of Cu(II) is 2 mg/L in drinking water and 0.05–1.5 mg/L in industrial effluent discharge [2]. Therefore, simple, green and high effective methods for Cu(II) removal are should be developed to guarantee the environmental safety and health.

Nowadays, a number of processes have been used to remove or eliminate heavy metal ions from wastewaters including chemical precipitation, electrochemical treatment, ion exchange, and chemical reduction [3–6]. However, these methods are not widely practical due to some drawbacks and limitations including high-energy consumption, high capital investment and running costs, generation of secondary toxic slurries and problems in the disposal of residual metal sludge [7,8]. The removal of Cu(II) from wastewaters by adsorption has attracted more and more researchers attention [9,10]. The main advantages of the adsorption process are high selectivity, less sludge volume produced, simplicity of design, a recovery of heavy metal and the meeting of strict discharge specification. Various materials such as clays, agricultural wastes, biomass, zeolite and synthetic polymers have been used as an adsorbent [11–15]. Recent studies have been focused on the development of cost-effective and efficient adsorbents. An efficient adsorptive material should consist of an insoluble porous matrix and some suitable active groups that can interact with heavy metal ions [16]. During the searching of new adsorption material for high metal ion uptake, composites were found to be most promising candidate because of its simple preparation, easy handling, low cost and excellent properties [17]. Owing to the faster diffusion rate of the metal ions into the internal binding sites in the porous adsorptive membrane than that of adsorptive beads, porous adsorptive membrane is now gaining more and more attention [18–21].

It is well known that biopolymers are abundant, biodegradable, non-toxic, renewable resources and can be modified in a number of ways to enhance their adsorption selectivity and efficiency. Meanwhile, use of biopolymers even makes the adsorption process more environmental friendly. Therefore, cost-effective biopolymers adsorbents have received increasing attention. Among them, polysaccharide type biopolymers such as chitosan [21,22], cellulose [23,24], cyclodextrin [25,26], sodium alginate [27–30] have received more attention. Sodium alginate (SA), for its good membrane forming property and high activity of carbonyl group and hydroxyl group on its chains which are excellent functional groups for anchoring heavy metals through chemical and physical interactions, has been preferred over other materials and attracted considerable attention currently [29,30].

Polyethyleneimine (PEI) is a kind of water-soluble polyamine, and the ratio of primary, secondary and ternary amine groups on their chains is equal to 1:2:1 approximately [31]. Therefore, PEI can produce very strong chelation ability toward heavy metal ions. PEI has been widely used for modifying various adsorbent, and its application in adsorption separation of heavy metal ions fields are investigating [32–34].

The objective of the present study was to prepare a novel porous membrane adsorbent (PEI/SA) by immobilizing PEI with SA using polyvinylpyrrolidone as a pore former, then functionalized with 3-aminopropyltriethoxysilane (APTEOS). The as-prepared porous membrane adsorbent (PEI/SA) combined the strong chelation ability of amino group towards Cu(II) and the fast diffusion rate of Cu(II) into the internal binding sites in the porous adsorptive membrane. Physico-chemical properties of the PEI/SA were investigated by using scanning electron microscopy (SEM), Fourier transformed infrared spectroscopy (FT-IR), thermogravimetric analysis (TG) and scanning probe microscope (AFM) methods. The PEI/SA was used for adsorption removal of Cu(II) from wastewater. Batch adsorption experiments were carried out to investigate the effects of adsorption factors, such as solution pH, adsorbent dose, initial Cu(II) ion concentration, adsorption temperature and contact time on adsorption property of the PEI/SA for Cu(II) ions. By testing various adsorption and kinetics models to fit our experimental data, we also studied the adsorption kinetics and isotherms of the PEI/SA for Cu(II). Meanwhile, the reusability of the PEI/SA for Cu(II) were also investigated.

2. Experimental section

2.1. Materials and analytical method

Sodium alginate (1.05–1.15 Pa s at 10 mg/L, Xilong Chemical Co. Ltd., China), polyethyleneimine ($M_w = 2 \times 10^4$–5×10^4, Qianglong Chemical Limited Company, China), copper nitrate, polyvinylpyrrolidone, hydrochloric acid, Sodium hydroxide (NaOH% ⩾96.0, Xilong Chemical Co. Ltd., China), γ-aminopropyl triethoxysilane (0.946 g/mL at 25 °C, Yaohua Chemical Co. Ltd., China), were purchased from Shanghai Chemical Reagent Store (Shanghai, China). All of them are of analytical grade and used without further purification.

A stock solution of 1000 mg/L of Cu(II) was prepared by dissolving certain amount of $Cu_2SO_4{\cdot}5H_2O$ in 1000 mL deionized water. A series of standard Cu(II) solutions were prepared by appropriate dilution of the stock Cu(II) solution. Solutions of 0.1 M NaOH and HCl were used for solution pH adjustment. The metal ions were determined using a flame atomic absorption spectroscopy (FAAS, GBC-932B, GBC Co. Ltd., Australia), equipped with air-acetylene flame.

2.2. Preparation of porous membrane adsorbent PEI/SA

Four grams of SA was dissolved in 400 mL deionized water following with the addition of 4.0 g PEI. To the above solution, 4.0 mL of 0.01 M HCl and 8.0 mL of APTEOS were dropwisely added in sequence under vigorous stirring with a blender (DSX-120, Hangzhou Electric Instrument Co, Ltd., China) at a speed of 500 rpm. Two hours later, 40.0 mL of aqueous polyvinylpyrrolidone (40.0 g/L) solution was mixed with the above solution under stirring till a homogeneous solution was obtained. The resulted solution was kept in a vacuum oven to remove bubbles, then was cast onto a glass plate (12 × 12 cm) and dried in an oven at 70 °C for 90 min. The dried membranes were carefully peeled off and immersed in fresh deionized water for 3 times (every time last 8 h). The resulted membranes were further dried in an oven at 70 °C for 180 min, and then stored in a desiccator for further experiments.

2.3. Membrane characterization

FT-IR spectra of the pristine PEI/SA porous membrane and Cu(II)-loaded PEI/SA porous membrane were scanned in the range from 4000 to 400 cm^{-1} by means of ATR-FTIR with an accumulation of 16 scans, resolution of 0.4 cm^{-1}, on a Nicolet-740.

The surface morphology of the pristine SA porous membrane and Cu(II)-loaded PEI/SA porous membrane were also characterized by SEM (Hitachi S-4800), equipped with an energy dispersive X-ray spectroscope, which was operated at EHT = 4.0 kV.

A CSPM-5500 scanning probe microscope (AFM, Benyuan, China) was used to carry out the morphological characterization of the pristine and Cu(II)-loaded PEI/SA porous membranes, operated in tapping mode. Tapping mode cantilevers (Tap300Al, Budget Sensors) with a spring constant of 40 N/m were used throughout the imaging.

The thermal properties of the pristine and Cu(II)-loaded PEI/SA porous membranes were analyzed using thermogravimetric analysis (Netzsch TG209 F1). Accurately weighted (8 mg) sample was

placed into aluminum cup and heated from room temperature to 800 °C at a constant heating rate 10 °C/min under constant nitrogen purging at 20 mL/min.

2.4. Batch adsorption studies

Batch adsorption studies were carried to determine the optimum conditions for the removal of copper ions from aqueous solution. Effect of the ratio of PEI to SA in the PEI/SA on adsorption was performed at adsorbent dose 0.5 g/L, solution pH 6, initial Cu(II) concentration 200 mg/L and adsorption temperature 30 °C for 60 min. Effect of solution pH on adsorption property was studied by varying the solution pH between 2 and 7, at an initial Cu(II) concentration 200 mg/L, adsorbent dosage 0.5 g/L and adsorption temperature 30 °C for 60 min. Effect of adsorbent dose on adsorption was carried out at adsorbent dose in the range of 0.1–2.0 g/L, initial Cu(II) concentration 200 mg/L, solution pH 6 and adsorption temperature 30 °C for 60 min. Effect of initial Cu(II) concentration on adsorption behavior was studied by varying Cu(II) concentrations in the range of 50 –1000 mg/L. These tests were performed at solution pH 6, adsorbent dose 0.5 g/L and adsorption temperature 30 °C for 60 min. Effect of adsorption temperature on adsorption was carried out at solution temperature in the range of 30–50 °C, initial Cu(II) concentration 200 mg/L, solution pH 6 and adsorbent dose 0.5 g/L for 60 min. Effect of contact time on adsorption behavior was studied in different time intervals ranging from 0 to 360 min. These tests were performed at solution pH 6, adsorbent dose 0.5 g/L, initial Cu (II) concentration 200 mg/L and adsorption temperature 30 °C.

Batch experiments were conducted by taking 300 mL Cu(II) solution in 500 mL reagent bottles at desired experimental conditions. The reagent bottles were placed on an orbital shaker running at 120 rpm until equilibrium was obtained. Five milliliters of the sample was drawn at regular intervals for heavy metal ions concentration testing. All the experiments were performed in triplicate and the average was taken for subsequent calculations.

The adsorption capacity of the adsorbent was evaluated by using the following expression:

$$q_t = \frac{(C_0 - C_t)V}{m} \quad (1)$$

where q_t is the mass of Cu(II) adsorbed per unit mass of the adsorbent, mg/g; V is the volume of the solution, L; m is the mass of the adsorbent, g; C_0 and C_t, are the concentration of Cu(II) in the initial aqueous solution and in the aqueous solution after adsorption for t min, mg/L, respectively.

The method used to investigate the point zero charge (PZC) of an adsorbent can be seen everywhere [35]. Briefly, in the present study, 50 mL of 0.1 M NaCl solution was transferred into a series of 100 mL volumetric flasks. The initial pH values (pH_I) of these solutions were adjusted from 1 to 8 by adding either 0.1 M HCl or 0.1 M NaOH solutions. Then, 0.10 g of PEI/SA was added into each flask. These flasks were placed on a shaker running at 150 rpm until the pH value of the two successive measurements was same. The difference between the initial pH value and equilibrium pH value (pH_E) ($\Delta pH = pH_I - pH_E$) was plotted against the pH_I. The value of horizontal abscissa of the resulting curve at which $\Delta pH = 0$ gave the PZC of the PEI/SA (Scheme 1).

2.5. Desorption of heavy metal ions and membrane reusability

Desorption of Cu(II) was carried out using 1.0 M HCl as a desorbing agent. The Cu(II)-loaded PEI/SA porous membrane samples were placed in a 250 mL desorption medium at 30 °C, with a shaking speed of 120 rpm for 60 min. The samples were washed with

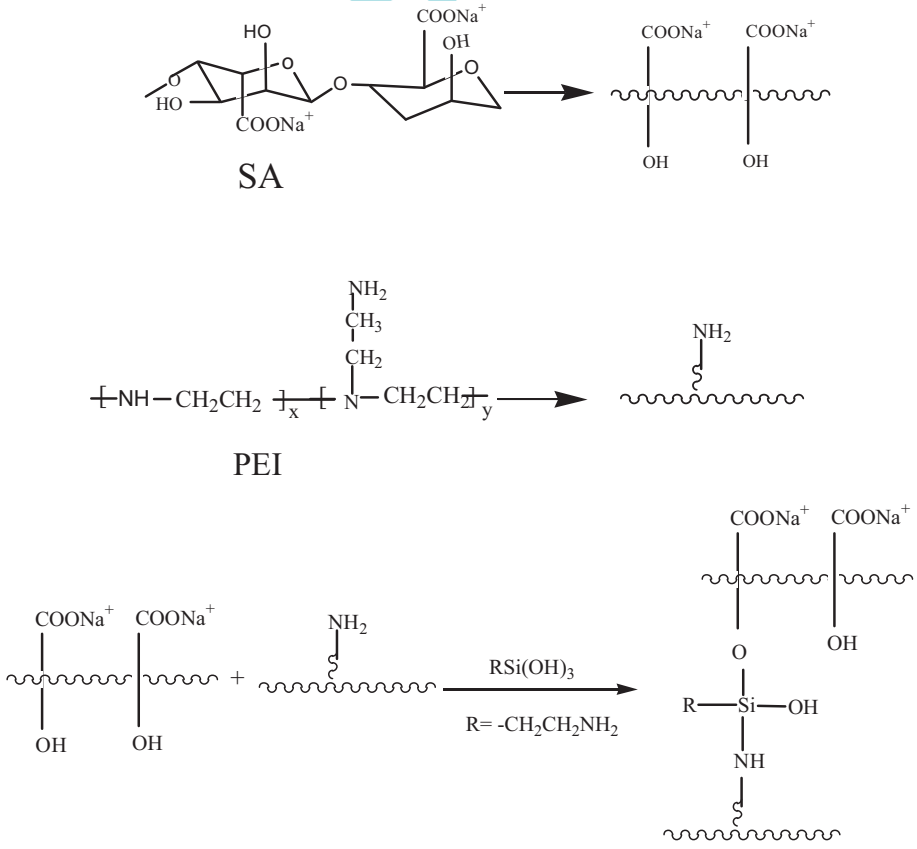

Scheme 1. Chemical structure and reaction model for cross-linking of SA and PEI.

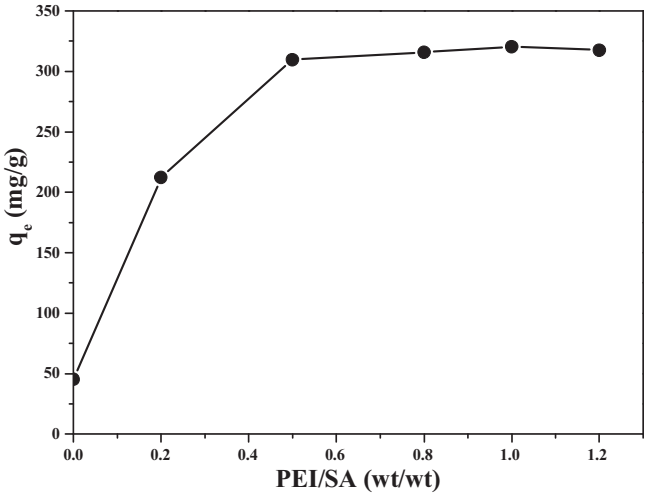

Fig. 1. Effect of the ratio of PEI to SA on adsorption.

deionized water several times and subjected again to adsorption/desorption process for eight cycles.

3. Results and discussion

3.1. Factors affecting adsorption efficiency

3.1.1. Effect of the addition ratio of PEI to SA on adsorption

Effect of the addition ratio of PEI to SA on adsorption property was performed under the following conditions: adsorbent dosage 0.5 g/L, solution pH 6, initial Cu(II) concentration 200 mg/L and adsorption temperature 30 °C for 60 min. From Fig. 1, we can observe that the effect of the rate PEI to SA on the adsorption capacity is significant, the saturated adsorption capacity of the PEI/SA for Cu(II) obtained the maximum when the rate PEI to SA is 1. As a result, the PEI/SA with PEI amount of 50 wt% was used for further adsorption experiments.

FT-IR spectra of pristine and Cu(II)-loaded PEI/SA porous membranes are presented in Fig. 2(a). It can be found that the spectrum of the pristine PEI/SA porous membrane exhibit a broad absorption band around 3268.46 cm^{-1} corresponding to O—H stretching vibrations of the hydroxyl group and N—H stretching vibrations of the amino group, which became weak after adsorption of Cu(II). This can be ascribed to the complexation of hydroxyl group and amino group with Cu(II). The band appearing at 1603.97 cm^{-1} has shifted to 1649.43 cm^{-1}, which can be attributed to the complexation of carboxylic group with Cu(II). The peaks observing at 1409.32 and 1091.76 cm^{-1} have shifted to 152.27 and 1195.48 cm^{-1} may also be attributed to the interaction of amino group with Cu(II).

Thermal properties of the pristine and Cu(II)-loaded PEI/SA porous membranes are presented in Fig. 2(b). As for pristine PEI/SA porous membrane, the first weight loss stage between 30 and 107 °C is associated with the evaporation of water adsorbed on the surface of PEI/SA; The second weight loss stage between 205 and 357 °C is attributed to the decomposition of $—NH_3^+$, $—COO^-$ and —OH groups of PEI/SA; and the next one higher than 452 °C can be attributed to the main chains depredation; Finally, when the temperature get 800 °C the residue is about 25.71 wt%, which can mainly be ascribed to SiO_2, the decomposing production of the APTEOS. From Fig. 2(b), we can observe that the thermal properties of the Cu(II)-loaded PEI/SA porous membrane is similar to that of the pristine PEI/SA porous membrane; however, the difference of the residue is about 9.17 wt%. This can mainly be attributed to the adsorption of copper species. Meanwhile, the increase in the thermal stability of membrane adsorbent at the temperature above 350 °C after the uptake of Cu (II) may be attributed to the interaction of amino group, hydroxyl group and carbonyl group with Cu(II).

SEM image, as shown in Fig. 3(a), shows that rough surface of the pristine PEI/SA porous membrane bears lots of tiny pores. Fig. 3(b) indicates that the reaction of Cu(II) with the amino group and hydroxyl group of the PEI/SA made the surface of PEI/SA porous membrane more roughness and protrusion. Meanwhile, the surface characteristic of the pristine and Cu(II)-loaded PEI/SA porous membranes were further investigated using an energy dispersive X-ray (EDX). From Fig. 3(c) and (d), one can find that the characteristic signal of Cu(II) could only be observed in the Fig. 3(d).

AFM is one of the most useful tools for investigating nanoscale surface topographies of the membrane. This technique gives a three-dimensional image for offering information concerning the

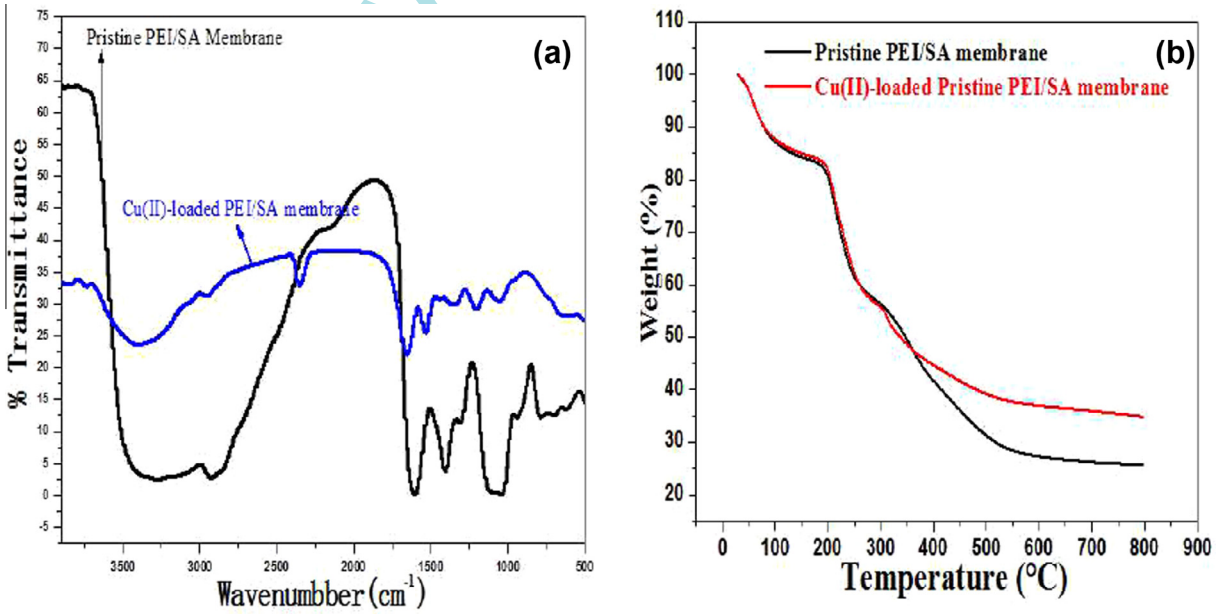

Fig. 2. (a) FT-IR spectra of pristine PEI/SA membrane and Cu(II)-loaded PEI/SA membrane; (b) TG analysis of pristine PEI/SA membrane and Cu(II)-loaded PEI/SA membrane.

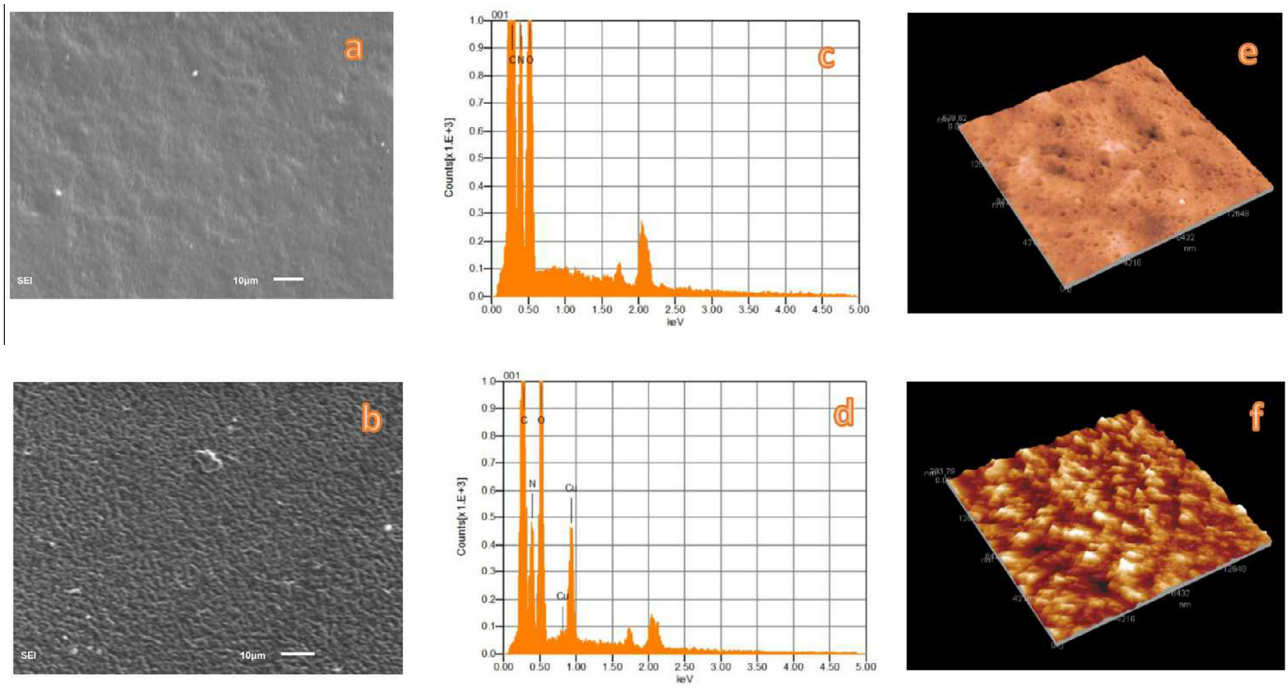

Fig. 3. (a) Pristine PEI/SA membrane (SEM); (b) Cu(II)-loaded PEI/SA membrane (SEM); energy dispersive X-ray analysis of: (c) pristine PEI/SA membrane (EDX); and (d) Cu (II)-loaded PEI/SA membrane (EDX); (e) pristine PEI/SA membrane (AFM); and (f) Cu(II)-loaded PEI/SA membrane (AFM).

changes in the surface roughness of a membrane adsorbent. Fig. 3 (e) and (f) presents AFM images of the pristine and Cu(II)-loaded PEI/SA porous membranes. Where the dark color zones represent depressions and light color regions correspond to the highest points on the surface of membrane. It can be observed that adsorption of Cu(II) by the $-NH_3^+$, $-COO^-$ and —OH group made the surface of PEI/SA porous membrane more coarse. The calculated roughness average (Ra) of the surfaces for the pristine and Cu(II)-loaded PEI/SA porous membranes are 15.38 nm and 24.23 nm, respectively.

3.1.2. Effects of solution pH on adsorption

Hydrogen ion concentration in solution is one of the most important parameters that influence adsorption behavior of metal ions in aqueous solutions. It affects the surface charge of an adsorbent, the solubility of metal ions in the solution and the degree of ionization of adsorbate during the reaction [36]. Meanwhile, hydrogen ion can strongly compete with positive metal ions for the adsorptive sites on the adsorbent. Thus, the solution pH can affect the adsorption property of an adsorbent. Effect of solution pH on adsorption is presented in Fig. 4. It indicates that adsorption capacity of the PEI/SA porous membrane for Cu(II) increases with an increasing of solution pH. This can be explained by the change in the ionic state of the amino group and carboxyl group on the adsorbent. When the solution pH is low, adsorptive functional groups are protonated, however, with an increasing of solution pH, amino group and carboxyl group are deprotonated and Cu(II) (principal species at solution pH value lower than 6) [37] can be bound to the negatively charged groups on the adsorbent. Since Cu(II) begin to precipitates when solution pH higher than 6.5 in the form of $Cu(OH)^{2+}$ [38]. Consequently, a solution pH 6 was chosen for further adsorption experiment.

The pH_{PZC} of a adsorbent corresponds to zero surface charge density, i.e. to equivalent amounts of negative and positive charges developed by proton equilibria. The pH_{PZC} of PEI/SA is 2.96. When the pH of Cu(II) solution is lower than the PZC, some of adsorptive groups such as hydroxy group, carbonyl group and amino group in the PEI/SA are protonated. As a result, the adsorptive sites of PEI/SA are positively charged, therefore induced electronic repulsion between Cu(II) and the adsorptive sites. While adsorptive sites on the surface of PEI/SA are negatively charged when the pH of Cu(II) solution is higher than the PZC, which favored positively charged Cu(II) adsorption on the surface of PEI/SA.

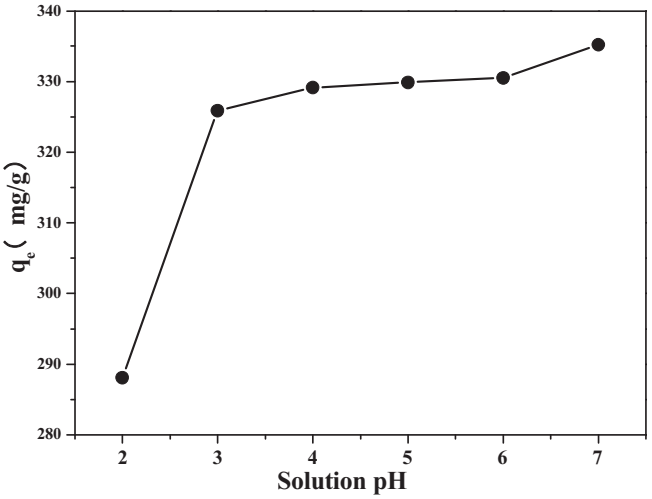

Fig. 4. Effect of solution pH on adsorption.

3.1.3. Effects of adsorbent dose on adsorption

Effect of adsorbent dose on adsorption results, as shown in Fig. 5, indicates that equilibrium adsorption capacity of the PEI/SA for Cu(II) decreases however Cu(II) removal efficiency increases with an increasing of adsorbent dose. It can be attributed to the fact that when more adsorbent dose was added some of the adsorption sites remain unsaturated during the adsorption process, and thus results in a lesser adsorption capacity.

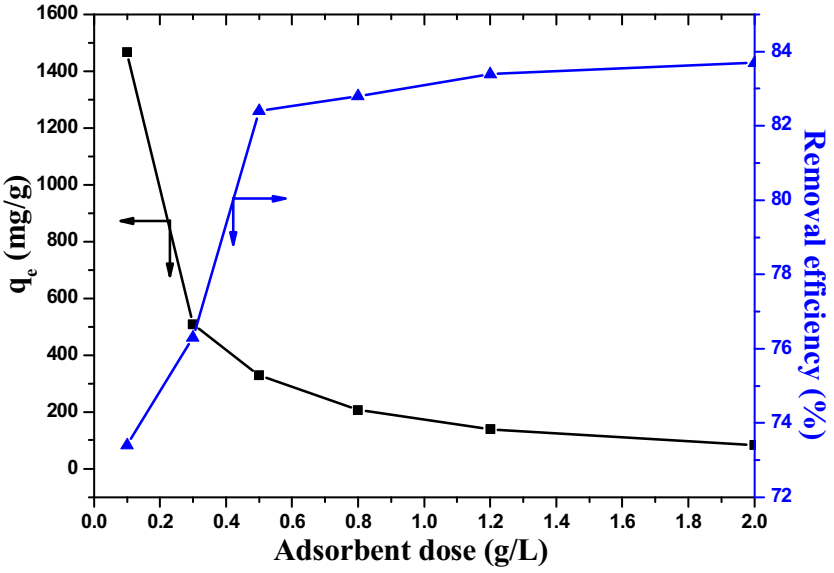

Fig. 5. Effect of adsorbent dose on adsorption.

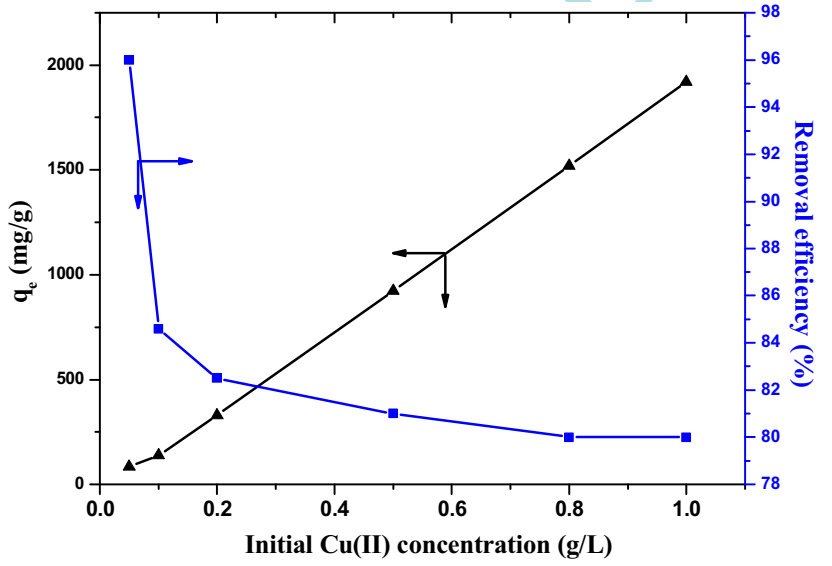

Fig. 6. Effect of initial Cu(II) concentration on adsorption.

3.1.4. Effects of initial Cu(II) concentration on adsorption

In batch adsorption processes, initial metal ion concentration provides an important driving force to overcome the mass transfer resistance of adsorbate between the aqueous solution and the adsorbent surface. As a result, the amount of adsorbate adsorbed is expected to be higher with a higher initial adsorbate concentration, hence improve the adsorption process. From Fig. 6, we observe that uptake capacity of the PEI/SA for Cu(II) increase with an increasing of Cu(II) concentration. This can be explained from the following two aspects: (1) higher initial Cu(II) concentration increases driving force to overcome the mass transfer resistance of Cu(II) between the aqueous and solid phases resulting in a higher probability of collision between Cu(II) and the adsorptive sites on the surface of PEI/SA; (2) an increasing of initial Cu(II) concentration may also led to a more intensity interaction between Cu (II) and PEI/SA, therefore enhance the availability of the adsorptive sites on the surface of PEI/SA.

3.1.5. Effects of temperature on adsorption

It has been recognized that the adsorption of heavy metal ions from an aqueous solution by adsorbent is affected by the temperature. An increasing in temperature is known to increase the diffusion rate of the adsorbate molecules across the external boundary layer and within the pores of the porous adsorbent. Furthermore, changing the temperature will modify the equilibrium capacity of the adsorbent for a particular adsorbate. Fig. 7 indicates that equilibrium adsorption capacity of the PEI/SA for Cu(II) increases slowly with a higher temperature. The result indicates the endothermic nature of the adsorption process. The increase in Cu(II) uptake capacity with a higher temperature can be explained from two aspects: (1) as the temperature rises, the diffusion of Cu (II) becomes much easier into the pore of PEI/SA because of the increase in the swelling degree of the PEI/SA. As a result, the adsorption capacity of the PEI/SA for Cu(II) increases; (2) bond rupture of the functional groups on the adsorbent surface at an elevated

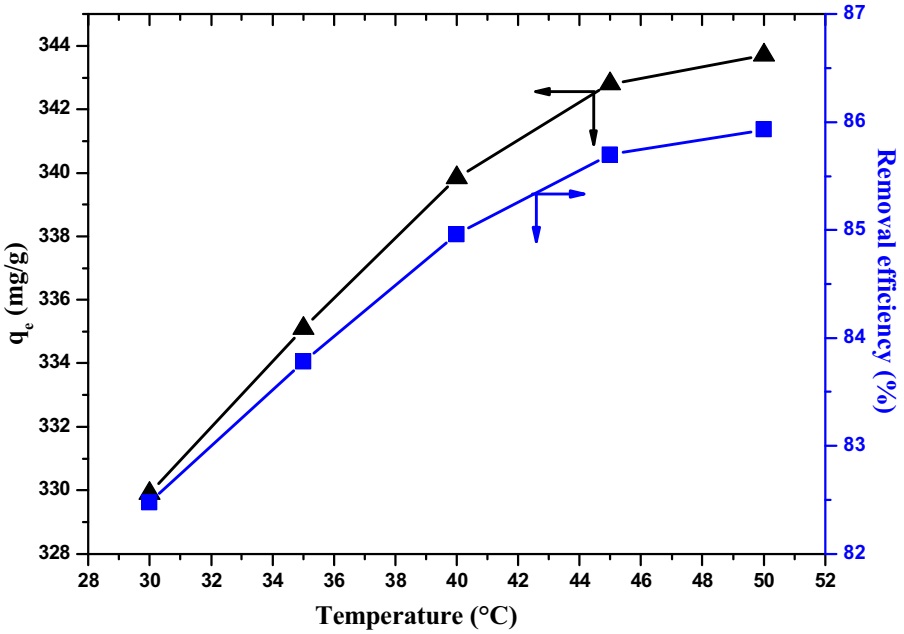

Fig. 7. Effects of temperature on adsorption.

temperature may increase the number of active adsorption sites, which may also lead to an enhanced adsorption capacity of the adsorbent.

3.1.6. Effect of contact time on adsorption

Effect of contact time on adsorption behavior is shown in Fig. 8. It indicates that the rate of Cu(II) adsorption onto the PEI/SA is very fast, where about 96.9% of the equilibrium adsorption capacity took place within the first 5 min and adsorption equilibrium is attained within 60 min. This is attributed to a large number of vacant surface adsorptive sites are available for adsorption during the initial stage, and with the lapse of time the available free surface is gradually filled up by the adsorbate species, adsorption process becomes slow and the kinetics may become more dependent on the rate at which the adsorbate molecules diffusion into the pore of the adsorbent and get adsorbed onto the surface of the inside pores. As a result, the adsorption experiments in the other parts were carried out for 60 min.

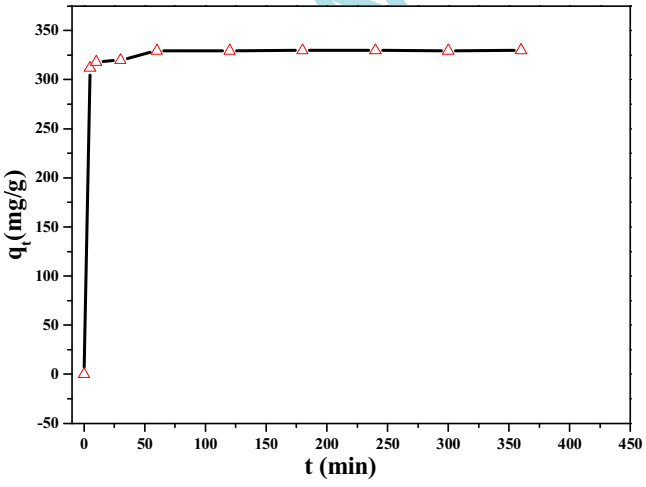

Fig. 8. Effects of contact time on adsorption.

3.1.7. Effect of ionic strength on adsorption

Generally, Na^+ and Ca^{2+} can be found in various industries wastewaters. The presence of Na^+ and Ca^{2+} ions leads to high ionic strength, which may significantly affect the behavior of the adsorption process. Adsorption experiments were carried out using NaCl and $CaCl_2$ as the ionic medium in the range of 0–1.2 mM/L to investigate the effect of ionic strength on adsorption property. These tests were carried out at initial Cu(II) concentration 200 mg/L, adsorbent dose 0.5 g/L, solution pH 6 and 30 °C for 60 min. Fig. 9 indicated that when the concentration of both electrolytes increased from 0 to 1.2 mM/L, the adsorption capacity of the PEI/SA for Cu(II) decreases from 329.9 mg/g to 324.1 mg/g for Na-electrolyte and from 329.9 mg/g to 306.7 mg/g for Ca-electrolyte, respectively. This can be attributed to Na^+ and Ca^{2+} can compete with Cu(II) for the same adsorption sites on the surface of the PEI/SA, thus negatively affect the adsorption capacity of the PEI/SA for Cu(II). Meanwhile, the increase in the concentration of chloride anions in solution has a possible formation of uncharged species ($CuCl_2$) and negatively charged chloride complexes ($CuCl_3^-$ and $CuCl_4^{2-}$) [39], which also reduce the adsorption performance of the PEI/SA. The adverse effect of the ionic strength on Cu(II) uptake suggests the possibility of ion exchange being involved in the adsorption process. However, form the Fig. 9, we observe that the adsorption processes are weakly affected by NaCl or $CaCl_2$ concentrations.

3.1.8. Coexisting metal ions

For the selective adsorption experiment, we used Cd(II), Ni(II) and Cr(VI) ions as the coexisting metal ions. The test was carried out at initial concentration of each metal ion 200 mg/L, solution pH 6, adsorbent dose 0.5 g/L and solution temperature 30 °C for 60 min. The results indicate that Cu(II) adsorption capacity by the PEI/SA is slightly affected, from 329.8 to 325.4 mg/g, under the presence of Ni(II), Cd(II) and Cr(VI) ions in the solution. The result could be attributed to the decrease in the number of binding site on the PEI/SA because co-existing ions competed with Cu(II) for adsorption site on the PEI/SA. However, the PEI/SA has much higher Cu(II) selectivity (325.4 mg/g) than that of Ni(II) (143.4 mg/g), Cd (II) (156.1 mg/g) and Cr(VI) (105.0 mg/g) ions in the solution. Cr

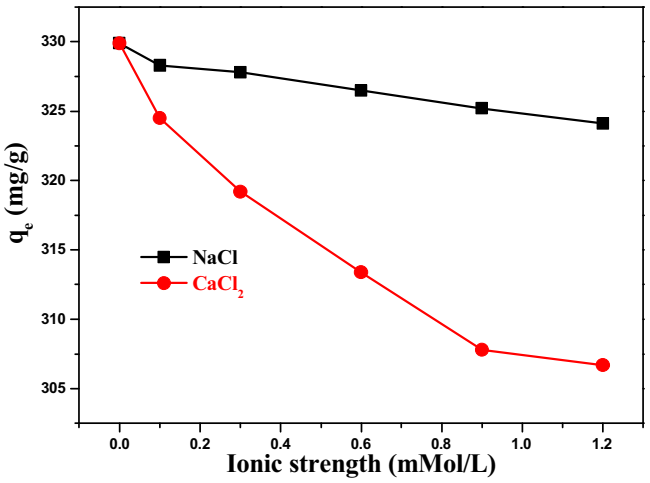

Fig. 9. Effect of ionic strength on adsorption.

(VI) ions mainly exists in various anionic forms, however, Cu(II), Cd (II) and Ni(II) exists in various cationic forms at solution pH 6 [40]. Meanwhile, the adsorptive sites of PEI/SA were negatively charged. As a result, the adsorption capacity of PEI/SA toward Cu(II), Cd(II) and Ni(II) is higher than that towards Cr(VI). Although the coordination of PEI with Cu(II), Cd(II) and Ni(II) ions has occurred, and the chelates with four ligands have been formed [41]. The adsorption capacities of Cu(II), Cd(II) and Ni(II) follow the order of Cu(II) > Cd (II) > Ni(II) maybe ascribed to the following factors: Firstly, the second ionization energy of Cu ($1.96 * 10^3$ kJ/mol) is far greater than those of Cd ($1.63 * 10^3$ kJ/mol) and Ni ($1.75 * 10^3$ kJ/mol), so Cu(II) accepts the electron pair of N atoms of ligand easily than Cd(II) and Ni(II). Secondly, the ionic radius of nickel is 0.69 A, and the ionic radius of cadmium is 0.97 A. Deformability of Cd(II) is greater than that of Ni(II), and Cd(II) is softer acid compared to Ni(II). Therefore, the adsorption capacity of the two kinds of ions on PEI/SA follows the order of Cd(II) > Ni(II).

3.2. Adsorption thermodynamic study

To investigate the mechanism involved in the adsorption, the thermodynamic behaviors of Cu(II) ion adsorption onto the PEI/SA porous membrane was evaluated employing the following equations:

$$K_d = \frac{(C_0 - C_e)}{C_e}\frac{V}{M} \tag{2}$$

$$\ln K_d = \frac{\Delta S^0}{R} - \frac{\Delta H^0}{RT} \tag{3}$$

$$\Delta G^0 = -RT \ln K_d \tag{4}$$

where, K_d is the distribution coefficient, (L/g); C_0 is the initial concentration, (mg/L); ΔH^0 is the enthalpy change, ΔS^0 is the entropy change and ΔG^0 is the Gibbs free energy change in a given process, kJ/mol, respectively.

Thermodynamic parameters were calculated according to Eqs. (2)–(4) and shown in Table 1. ΔG^0 values are negative for Cu(II) adsorption onto the PEI/SA indicate that adsorption is spontaneous. These values decrease with an increase of temperature indicating a better adsorption performance can be obtained at higher temperature. The positive values of ΔH^0 confirm the endothermic nature of the overall adsorption process. The positive value of ΔS^0 suggests an increased randomness at the solid/solution interface.

3.3. Adsorption kinetics and isotherms study

3.3.1. Adsorption kinetics study

To examine the mechanism of adsorption processes, we tested the Lagergren pseudo-first-order kinetic model and pseudo-second-order kinetic model, the intra-particular diffusion model and the Crank model [42] with our experiments data.

(1) Lagergren pseudo-first-order kinetic model:

$$\ln(q_e - q_t) = \ln q_e - k_1 t \tag{5}$$

(2) pseudo-second-order kinetic model:

Table 1
Thermodynamic parameters calculated for Cu(II) adsorption onto the PEI/SA: adsorbent dose 0.5 g/L; Cu(II) concentration 200 mg/L; solution pH 6; speed agitation 120 rpm; and time 60 min.

Adsorbent	ΔH^0 (kJ/mol)	ΔS^0 (kJ/mol)	$-\Delta G^0$ (kJ/mol)				
			303.15(K)	308.15(K)	313.15(K)	318.15(K)	323.15(K)
PEI/SA	11.542	56.813	5.652	5.974	6.317	6.578	6.736

Table 2
The Lagergren pseudo-first-order model, the Lagergren pseudo-second-order model, intra-particle diffusion model and Crank model parameters for Cu(II) ions adsorption onto the PEI/SA: adsorbent dose 0.5 g/L; Cu(II) concentration 200 mg/L; pH 6.0; speed agitation 120 rpm; and time 60 min.

Models	q_e (mg/g)	Parameters			R^2
Pseudo-first-order	329.9	k_1 (min^{-1}) 0.734	$q_{e,c}$ (mg/g) 319.91		0.8530
Pseudo-second-order	329.9	k_2 (g/mg min) 4.89×10^{-4}	$q_{e,c}$ (mg/g) 327.58		0.9999
Intra-particle diffusion model		K_{dif1} (mg/g $min^{-1/2}$) 139.46 K_{dif2} (mg/g $min^{-1/2}$) 1.75	C_1 0 C_2 316.42		1.00 0.99
Crank model		$k_f \times 10^{-4}$ (m/s) 2.72	$D_s \times 10^{-12}$ (m^2 s) 4.95	Biot 126	

$$\frac{t}{q_t} = \left(\frac{1}{k_2 q_e^2}\right) + \frac{t}{q_e} \quad (6)$$

where q_e and q_t denote the amounts of adsorption per unit mass of the adsorbent at equilibrium and at time t (mg/g); k_1 and k_2 are the first order and second order rate constants (1/min), respectively.

The relevant parameters are shown in Table 2. It is observed that the pseudo-second-order equation appears to be the better-fitting model because it has the higher R^2 (0.9999); Meanwhile, the calculated amount of adsorption equilibrium ($q_{e,c}$, 327.58) from pseudo-second-order equation is close to the actual amount of adsorption equilibrium (q_e, 329.9).

(3) Furthermore, the intra-particle diffusion kinetic model based on the equation proposed by Weber and Morris was tested. This empirical equation assumes that adsorbate uptake by adsorbent varies almost proportionally with $t^{1/2}$ rather than with the contact time t. According to the following Weber–Morris's equation [43]:

$$q_t = k_{dif} t^{1/2} + C_i \quad (7)$$

where q_t is the amounts of adsorption at time t (mg/g), and k_{dif} is the intra-particular diffusion rate constant (mg/g $\text{min}^{1/2}$). C_i is the intercept of stage i, giving an idea about the thickness of boundary layer, that is, the larger the intercept, the greater the boundary layer effect.

The relation plots of q_t versus time $t^{1/2}$ is shown in Fig. 10. It shows that the plots is not linear over the whole time range and can be separated into two linear regions which confirm the multi-stages of adsorption. Stage **I** is rapidly completed within about 5 min and the stage of intraparticle diffusion control (stage **II**) is then attained. It may be concluded that surface adsorption and intra-particle diffusion are concurrently happened in the present study. The first stage is characterized by physical adsorption of the PEI/SA functional groups and the second stage is due to the intra-particle diffusion effects. The rate parameters for intra-particular diffusion model, as shown in Table 2, indicate that the order of uptake rate is as follows: $K_{dif1} > K_{dif2}$, possibly because the concentration of Cu(II) left in the solutions gradually decreases and diffusion resistance originate from adsorbate diffusion through the hole in the particles into particles inside.

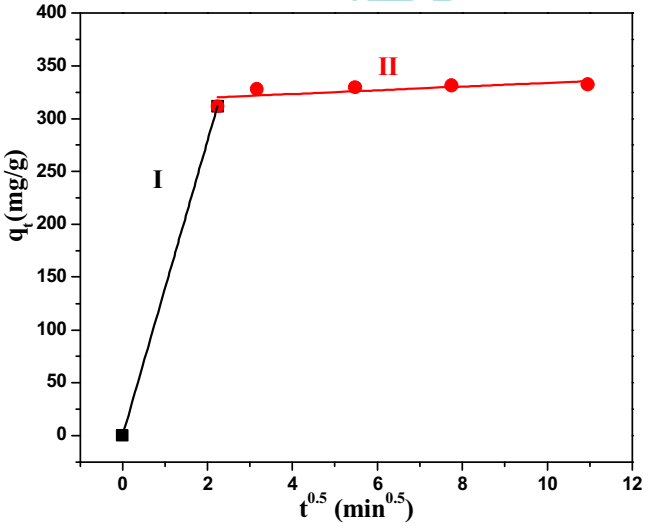

Fig. 10. Investigate intra-particular diffusion model for Cu(II) adsorption onto the PEI/SA membrane.

(4) Crank model

According to the Crank diffusion model, mass transfer rate of Cu(II), N_t, at the external surface of adsorbent can be described as follows:

$$N_t = \frac{\partial C_t}{\partial t} = k_f S_A (C_t - C_s) \quad (8)$$

Integrating Eq. (8), the following expression is obtained:

$$\ln\left(\frac{C_t}{C_0}\right) = -k_f S_A t \quad (9)$$

where C_t is bulk liquid phase concentration, mg/L; C_s is liquid phase concentration at the surface in equilibrium with the solid phase concentration, mg/L; k_f is an external mass transfer coefficient, m/s; S_A is the specific surface area of adsorbent, m^2/g.

Crank also developed the following equation for a slab particle, which can also be used for membrane adsorbent [44]:

$$\frac{q_t}{q_e} = 1 - \sum_{n=1}^{\infty} \frac{6}{\pi^2 n^2} \times \exp\left(\frac{-n^2 \pi^2 D_S t}{r^2}\right) \quad (10)$$

where D_S is the effective intra-particle diffusion coefficient of the adsorbent in the particle, m^2/s.

The Biot number, B_i (dimensionless), could be calculated as below:

$$B_i = \frac{k_f L_f}{D_S} \quad (11)$$

where, L_f is the thickness of the film (or membrane).

The B_i values calculated with experimental data are presented in Table 2. It indicates that the B_i value is significant higher than one, which suggests that the adsorption process is mainly controlled by the intra-particle diffusion [45].

3.3.2. Adsorption isotherms study

In an adsorption system, the adsorption results in the removal of solute from the solution onto the adsorbent surface until the remaining solute in the solution is in dynamic equilibrium with solute on the adsorbent surface. A plot of the solute concentration in the adsorbent phase q_e (mg/g) as function of the solute concentration in the solution C_e (mg/L) at equilibrium gives an adsorption isotherm. An adsorption isotherm can be utilized to obtain information about the interaction between the adsorbent and adsorbate molecules. In order to understand and clarify the adsorption process, Langmuir adsorption isotherm and Freundlich adsorption isotherm models were applied in this study.

The Langmuir adsorption isotherm equation is an often used adsorption model of completely homogenous surface with negligible interaction between adsorbed molecules, shown as below:

$$\frac{C_e}{q_e} = \frac{1}{b q_{\max}} + \frac{C_e}{q_{\max}} \quad (12)$$

where q_e is the amounts of adsorption at equilibrium (mg/g), C_e is the equilibrium concentration of the adsorbate in the solution (mg/L). q_{max} is the adsorption capacity (mg/g), and b is the adsorption intensity or Langmuir coefficient related to the affinity of the binding site (L/mg).

The Freundlich adsorption isotherm equation is a purely empirical relationship based on heterogeneous surfaces suggesting that binding sites are not equivalent and independent. The Freundlich adsorption isotherm equation can be expressed as follows:

$$\ln q_e = \ln K_F + 1/n \ln C_e \quad (13)$$

Table 3
Kinetic data from the Langmuir isotherm and the Freundlich isotherm: adsorbent dosage 0.5 g/L; temperature 30 °C; pH 6.0; speed agitation 120 rpm; and time 60 min.

Langmuir q_{max} (mg/g)	Isotherm b (L/mg)	Parameters R^2	Freundlich K_F (mg/g)	Isotherm n	Parameters R^2
2638	171.5	0.6938	30.56	1.38	0.9982

Table 4
Comparison of maximum adsorption capacities of various adsorbents for Cu(II) ions.

Adsorbent	Maximum adsorption capacity (mg/g)	References
Corn stalk	20.6	[2]
Composite adsorbent	200.8	[3]
GO/CdS(en)	132.4	[4]
Facial composite adsorbent	176.3	[8]
Cinnamomum camphora leaves powder	17.9	[9]
Bofe calcined clay	19.2	[11]
Raw shell	3.3	[12]
Modified litchi pericarp	23.7	[13]
Ion-imprinted polymers acrylamide and triethylene glycol divinyl ether	41.0	[14]
GA-HA/SA	63.1	[20]
Polyazomethineamides	470.7	[37]
Maple wood sawdust	9.5	[38]
Cu–PVA–SA	79.3	[43]
PEI/SA	329.8	Present work

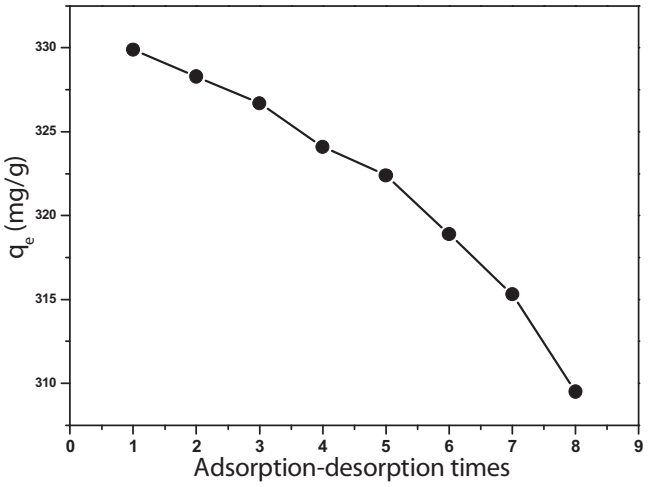

Fig. 11. Adsorption–desorption cycles.

where K_F and $1/n$ are the constants that are related to the adsorption capacity and the adsorption intensity, respectively. A smaller $1/n$ value indicates a more heterogeneous surface whereas a value closer to or equal to one indicates the adsorbent has relatively more homogeneous binding sites.

The isotherm constants were calculated from the experimental data and presented in Table 3. Taken into consideration the values of the correlation coefficient as a criterion for goodness of fit for the system, the Freundlich isotherm model shows better correlation (R^2 = 0.9982) than the Langmuir isotherm model (R^2 = 0.6938), which indicates that the Freundlich adsorption isotherm model represents the adsorption process more ideally. It also suggests the heterogeneous nature of adsorptive sites on the surface of the PEI/SA.

3.4. Comparison of various adsorbents for Cu(II) ions adsorption

Table 4 presents a comparison of maximum Cu(II) ions adsorption capacity between PEI/SA and various type of adsorbents. It obvious that the Cu(II) ions uptake capacity of PEI/SA in this work has encouraging adsorption capacity.

3.5. Desorption of heavy metal ions and reusability

Reusability is an important factor for an adsorbent because it will reduce the overall cost of the applied adsorbent. The consecutive adsorption–desorption experiments are presented in Fig. 11, which indicates the adsorption capacity of the PEI/SA for Cu(II) after eight cycles still remains 94.1% of its original adsorption capacity. The result indicates that the prepared PEI/SA can be effectively used for treatment wastewater containing Cu(II).

4. Conclusion

In the present paper, a novel porous membrane adsorbent PEI/SA with excellent adsorption property was prepared. Cu(II) adsorption on the PEI/SA is weakly dependent on solution pH, adsorption temperature and ionic strength. The adsorption rate of PEI/SA for Cu(II) is fast and adsorption equilibrium is obtained within 60 min. The maximum uptake capacity of the PEI/SA for Cu(II) under the optimal condition is 329.9 mg/g. The kinetics adsorption data could be well fitted with pseudo-second-order kinetic model. Meanwhile, the kinetic experiment results also indicate that the rate of controlling step is mainly intra-particle diffusion but is not the only rate-limiting step for Cu(II) adsorption. The equilibrium data can be well fitted with the Freundlich isotherm model. After eight cycles of adsorption–desorption experiments, the adsorption capacity is still considerable. Based on the experiment results, the prepared PEI/SA porous membrane can be used as a cost-effective, easy operation and efficient adsorbent for removing Cu(II) from wastewaters.

Acknowledgements

The authors would like to acknowledge the financial support of this work from National Natural Science Foundation of China (No. 21076174), Natural Science Foundation of Fujian (2012J06005 and 2014J01051), and the Science and Technology Key Project of Fujian (2013H0053). The authors also thank the anonymous referees for comments on this manuscript.

References

[1] D. Gusain, V. Srivastava, Y.C. Sharma, Kinetic and thermodynamic studies on the removal of Cu(II) ions from aqueous solutions by adsorption on modified sand, J. Ind. Eng. Chem. 20 (2014) 841–847.
[2] S. Vafakhah, M.E. Bahrololoom, R. Bazarganlari, M. Saeedikhani, Removal of copper ions from electroplating effluent solutions with native corn cob and corn stalk and chemically modified corn stalk, J. Environ. Chem. Eng. 2 (2014) 356–361.
[3] M.R. Awual, M.M. Hasan, Colorimetric detection and removal of copper(II) ions from wastewater samples using tailor-made composite adsorbent, Sens. Actuators, B 206 (2015) 692–700.
[4] T.S. Jiang, W.P. Liu, Y.L. Mao, L. Zhang, J.L. Cheng, M. Gong, H.B. Zhao, L.M. Dai, S. Zhang, Q. Zhao, Adsorption behavior of copper ions from aqueous solution onto graphene oxide-CdS composite, Chem. Eng. J. 259 (2015) 603–610.
[5] F. Fang, L.T. Kong, J.R. Huang, S.B. Wu, K.S. Zhang, X.L. Wang, B. Sun, Z. Jin, J. Wang, X.J. Huang, J.H. Liu, Removal of cobalt ions from aqueous solution by an amination graphene oxide nanocomposite, J. Hazard. Mater. 270 (2014) 1–10.
[6] C. Ling, F.Q. Liu, C. Long, T.P. Chen, Q.Y. Wu, A.M. Li, Synergic removal and sequential recovery of acid black 1 and copper(II) with hyper-crosslinked resin and inside mechanisms, Chem. Eng. J. 236 (2014) 323–331.
[7] D. Kolodynska, The effect of the novel complexing agent in removal of heavy metal ions from waters and waste waters, Chem. Eng. J. 165 (2010) 835–845.

[8] M.R. Awual, A novel facial composite adsorbent for enhanced copper(II) detection and removal from wastewater, Chem. Eng. J. 266 (2015) 368–375.
[9] H. Chen, G.L. Dai, J. Zhao, A.G. Zhong, J.Y. Wu, H. Yan, Removal of copper(II) ions by a biosorbent-*Cinnamomum camphora* leaves powder, J. Hazard. Mater. 177 (2010) 228–236.
[10] Z.H. Cheng, X.S. Liu, M. Han, W. Ma, Adsorption kinetic character of copper ions onto a modified chitosan transparent thin membrane from aqueous solution, J. Hazard. Mater. 182 (2010) 408–415.
[11] A.F.D.A. Neto, M.G.A. Vieira, M.G.C.D. Silva, Adsorption and desorption processes for copper removal from water using different eluents and calcined clay as adsorbent, J. Water Process Eng. 3 (2014) 90–97.
[12] Q. Wu, J. Chen, M. Clark, Y. Yu, Adsorption of copper to different biogenic oyster shell structures, Appl. Surf. Sci. 311 (2014) 264–272.
[13] Z.L. Kong, X.C. Li, J.Y. Tian, J.L. Yang, S.J. Sun, Comparative study on the adsorption capacity of raw and modified litchi pericarp for removing Cu(II) from solutions, J. Environ. Manage. 134 (2014) 109–116.
[14] J.J. Wang, L. Ding, J. Wei, F. Liu, Adsorption of copper ions by ion-imprinted simultaneous interpenetrating network hydrogel: thermodynamics, morphology and mechanism, Appl. Surf. Sci. 305 (2014) 412–418.
[15] M. Mercurio, V. Mercurio, B. De' Gennaro, M. De' Gennaro, C. Grifa, A. Langella, V. Morra, Natural zeolites and white wines from Campania region (Southern Italy): a new contribution for solving some oenological problems, Per. Mineral. 79 (2010) 95–112.
[16] G.J. Copello, L.E. Diaz, V.C. Dall'Orto, Adsorption of Cd(II) and Pb(II) onto a one step-synthesized polyampholyte: kinetics and equilibrium studies, J. Hazard. Mater. 217–218 (2012) 374–381.
[17] S.B. Khan, J.W. Lee, H.M. Marwani, K. Akhtar, A.M. Asiri, J. Seo, A.A.P. Khan, H. Han, Polybenzimidazole hybrid membranes as a selective adsorbent of Mercury, Compos. B 56 (2014) 392–396.
[18] C.X. Liu, R.B. Bai, Adsorptive removal of copper ions with highly porous chitosan/cellulose acetate blend hollow fiber membranes, J. Membr. Sci. 284 (2006) 313–322.
[19] M.M. Nasef, A.H. Yahaya, Adsorption of some heavy metal ions from aqueous solutions on Naf ion 117 membrane, Desalination 249 (2009) 677–681.
[20] J.H. Chen, Q.L. Liu, S.R. Hu, J.C. Ni, Y.S. He, Adsorption mechanism of Cu(II) ions from aqueous solution by glutaraldehyde crosslinked humic acid-immobilized sodium alginate porous membrane adsorbent, Chem. Eng. J. 73 (2011) 511–519.
[21] L.L. Min, Z.H. Yuan, L.B. Zhong, Q. Liu, R.X. Wu, Y.M. Zheng, Preparation of chitosan based electrospun nanofiber membrane and its adsorptive removal of arsenate from aqueous solution, Chem. Eng. J. 267 (2015) 132–141.
[22] L. Li, Y.X. Li, L.X. Cao, C.F. Yang, Enhanced chromium(VI) adsorption using nanosized chitosan fibers tailored by electrospinning, Carbohydr. Polym. 125 (2015) 206–213.
[23] Z.J. He, H. Song, Y.N. Cui, W.X. Zhu, K.F. Du, S. Yao, Porous spherical cellulose carrier modified with polyethyleneimine and its adsorption for Cr(III) and Fe (III) from aqueous solutions, Chinese J. Chem. Eng. 22 (2014) 984–990.
[24] J. Yang, F. Kubota, Y. Baba, N. Kamiya, M. Goto, Application of cellulose acetate to the selective adsorption and recovery of Au(III), Carbohyd. Polym. 111 (2014) 768–774.
[25] W. Liu, X.Y. Jiang, X.Q. Chen, A novel method of synthesizing cyclodextrin grafted multiwall carbon nanotubes/iron oxides and its adsorption of organic pollutant, Appl. Surf. Sci. 320 (2014) 764–771.
[26] J.S. Liu, G.N. Liu, W.X. Liu, Preparation of water-soluble b-cyclodextrin/poly(acrylic acid)/grapheme oxide nanocomposites as new adsorbents to remove cationic dyes from aqueous solutions, Chem. Eng. J. 257 (2014) 299–308.
[27] R. Bhattacharyya, S.K. Ray, Adsorption of industrial dyes by semi-IPN hydrogels of acrylic copolymers and sodium alginate, J. Ind. Eng. Chem. 22 (2015) 92–102.
[28] R. Karthik, S. Meenakshi, Removal of Cr(VI) ions by adsorption onto sodium alginate-polyaniline, Int. J. Biol. Macromol. 72 (2015) 711–717.
[29] M.M. Lakouraj, F. Mojerlou, E.N. Zare, Nanogel and superparamagnetic nanocomposite based on sodium alginate for sorption of heavy metal ions, Carbohyd. Polym. 106 (2014) 34–41.
[30] V. Dhanapala, K. Subramanian, Recycling of textile dye using double network polymer from sodium alginate and superabsorbent polymer, Carbohyd. Polym. 108 (2014) 65–74.
[31] B.J. Gao, Y.B. Li, Z.P. Chen, Adsorption behaviour of functional grafting particles based on polyethyleneimine for chromate anions, Chem. Eng. J. 150 (2009) 337–343.
[32] M. Owlad, M.K. Aroua, W.M.W. Daud, Hexavalent chromium adsorption on impregnated palm shell activated carbon with polyethyleneimine, Bioresource Technol. 101 (2010) 5098–5103.
[33] C.Y. Yin, M.K. Aroua, W.M.A.W. Daud, Impregnation of palm shell activated carbon with polyethyleneimine and its effects on Cd^{2+} adsorption, Colloids Surf. A: Physicochem. Eng. Asp. 307 (2007) 128–136.
[34] B.J. Gao, F.Q. An, K.K. Liu, Studies on chelating adsorption properties of novel composite material polyethyleneimine/silica gel for heavy-metal ions, Appl. Surf. Sci. 253 (2006) 1946–1952.
[35] K.S. Tong, M. Jain Kassim, A. Azraa, Adsorption of copper ion from its aqueous solution by a novel biosorbent *Uncaria gambir*: equilibrium, kinetics, and thermodynamic studies, Chem. Eng. J. 170 (2011) 145–153.
[36] S.M. Nomanbhay, K. Palanisamy, Removal of heavy metals from industrial wastewater using chitosan coated oil palm shell charcoal, Electron. J. Biotechnol. 8 (2004) 43–53.
[37] A. Murugesan, L. Ravikumar, V. SathyaSelvaBala, P. SenthilKumar, T. Vidhyadevi, S.D. Kirupha, S.S. Kalaivani, S. Krithig, S. Sivanesan, Removal of Pb(II) Cu(II) and Cd(II) ions from aqueous solution using polyazomethineamides: equilibrium and kinetic approach, Desalination 271 (2011) 199–208.
[38] M.S. Rahmana, M.R. Islam, Effects of pH on isotherms modeling for Cu(II) ions adsorption using maple wood sawdust, Chem. Eng. J. 149 (2009) 273–280.
[39] T.S. Anirudhan, P.G. Radhakrishnan, Chromium (III) removal from water and wastewater using a carboxylate-functionalized cation exchanger prepared from a lignocellulosic residue, J. Colloid Interface Sci. 316 (2007) 268–276.
[40] J.H. Chen, H.T. Xing, H.X. Guo, W. Weng, S.R. Hu, S.X. Li, Y.H. Huang, X. Sun, Z.B. Su, Investigation on the adsorption properties of Cr(VI) ions on a novel graphene oxide (GO) based composite adsorbent, J. Mater. Chem. A 2 (2014) 12561–12570.
[41] B.J. Gao, F.Q. An, K.K. Liu, Studies on chelating adsorption properties of novel composite material polyethyleneimine/silica gel for heavy-metal ions, Appl. Surf. Sci. 253 (2006) 1946–1952.
[42] C.O. Illanes, N.A. Ochoa, J. Marchese, Kinetic sorption of Cr(VI) into solvent impregnated porous microspheres, Chem. Eng. J. 136 (2008) 92–98.
[43] W.J. Weber, J.C. Morris, Advances in water pollution research: removal of biologically resistant pollutants from waste waters by adsorption, in: Proceedings of International Conference on Water Pollution Symposium, vol. 2, Pergamon, Oxford, 1962, pp. 231–266.
[44] P.W. Majsztrik, M.B. Satterfield, A.B. Bocarsly, J.B. Benziger, Water sorption, desorption and transport in Nafion membranes, J. Membr. Sci. 301 (2007) 93–106.
[45] J.H. Chen, H. Lin, Z.H. Luo, Y.S. He, Cu(II)-imprinted porous film adsorbent Cu–PVA–SA has high uptake capacity for removal of Cu(II) ions from aqueous solution, Desalination 277 (2011) 265–273.